International Journal of Bifurcation and Chaos, Vol. 22, No. 6 (2012) 1250139 (11 pages)

DOI: 10.1142/S0218127412501398

# AN EFFICIENT AND ACCURATE NUMERICAL SCHEME FOR TURING INSTABILITY ON A PREDATOR–PREY MODEL

ANA YUN, DARAE JEONG and JUNSEOK KIM*
*Department of Mathematics, Korea University,*
*Seoul 136-701, Seoul, Korea*
**cfdkim@korea.ac.kr*

Received February 28, 2011; Revised June 10, 2011

We present an efficient and accurate numerical method for solving a ratio-dependent predator–prey model with a Turing instability. The system is discretized by a finite difference method with a semi-implicit scheme which allows much larger time step sizes than those required by a standard explicit scheme. A proof is given for the positivity and boundedness of the numerical solutions depending only on the temporal, but not on the spatial step sizes. Finally, we perform numerical experiments demonstrating the robustness and accuracy of the numerical solution for the Turing instability. In particular, we show that the numerical nonconstant stationary solutions exist.

*Keywords*: Turing instability; ratio-dependent predator–prey; semi-implicit scheme.

## 1. Introduction

A predator–prey model which considers the predator's growth rate as a function of the ratio of prey to predator abundance ratio is called the ratio-dependent model which seems more appropriate theoretically and empirically [Arditi & Ginzburg, 1989; Kuang & Beretta, 1998; Wang *et al.*, 2007]. We consider a ratio-dependent model, especially having a Turing instability. The Turing instability means that the equilibrium solution is asymptotically stable in the kinetic system (without diffusion), however it is unstable with a diffusion term. The Turing instability has been extensively investigated for biological and chemical processes [Tapaswi & Chattopadhyay, 1993; Shiferaw & Karma, 2006; Nakao & Mikhailov, 2010]. Moreover, pattern formation from the Turing instability in nonlinear complex systems is actively investigated in the fields such as social networks, molecular computing, and mathematics [Medvinsky *et al.*, 2002; Calude & Păun, 2004; McGehee *et al.*, 2008]. In this paper, we focus on the efficient and accurate numerical scheme for a reaction–diffusion system, especially a ratio-dependent model with a Turing instability.

The typical model for a predator–prey system is a simple Holling Type II [Holling, 1959; Peng *et al.*, 2009] which has a constant mortality of the predator. McGehee *et al.* [2008] introduced a more realistic model which considers the predator mortality as an increasing function of the predator's abundance. We use the modified Cavani and Farkas model [Cavani & Farkas, 1994a, 1994b] proposed by Aly *et al.* [2011], which is a ratio-dependent model with diffusion and without delay.

Let $N(x, t)$ and $P(x, t)$ be the prey and predator population densities for space $x$ on the one-dimensional domain $\Omega = (0, l)$ and time $t$,

*Author for correspondence

respectively. The governing equations are:

$$N_t = rN\left(1 - \frac{N}{K}\right) - \frac{aNP}{mP + N} + D_1 N_{xx}, \quad (1)$$

$$P_t = -\frac{P(\gamma + \delta P)}{1 + P} + \frac{bNP}{mP + N} + D_2 P_{xx}, \quad (2)$$

where $a$, $b$, $r$, $m$, $\gamma$, $\delta$, $D_1$, $D_2$ and $K$ are positive constants. Subscripts denote partial differentiation with respect to the variables.

The prey grows with the intrinsic growth rate $r$ and the constant carrying capacity $K$. The presence of the predator reduces the prey's growth rate with a capturing rate $a$ and a capturing time related to a factor $mP$. The predator's mortality is $(\gamma + \delta P)/(1+P)$, where $\gamma$ and $\delta$ are the minimal and limiting mortalities of the predator, respectively. Naturally, we can assume that $0 < \gamma \leq \delta$. Also, the prey's contribution to the predator's growth rate is $bNP/(mP + N)$, where $b$ is a conversion rate. Assume that the prey and predator diffuse by Fick's law with constant diffusions $D_1$ and $D_2$. The boundary conditions satisfy the homogeneous Neumann boundary conditions:

$$N_x(0,t) = N_x(l,t) = P_x(0,t) = P_x(l,t) = 0$$

and initial conditions are given by $N(x,0) > 0$, $P(x,0) > 0$, $x \in (0,l)$. The governing Eqs. (1) and (2) can be nondimensionalized by introducing dimensionless variables

$$\tilde{t} = rt, \quad \tilde{N} = \frac{N}{K}, \quad \tilde{P} = \frac{mP}{K}, \quad \tilde{x} = \frac{x}{l},$$

$$\alpha = \frac{a}{mr}, \quad \tilde{\gamma} = \frac{\gamma}{b}, \quad \tilde{\delta} = \frac{\delta}{b}, \quad \epsilon = \frac{b}{r},$$

$$\beta = \frac{K}{r}, \quad d_1 = \frac{D_1}{l^2 r}, \quad d_2 = \frac{D_2}{l^2 r}.$$

After omitting tilde notation, we get the following nondimensional system:

$$N_t = N(1 - N) - \frac{\alpha NP}{P + N} + d_1 N_{xx}, \quad (3)$$

$$P_t = -\frac{\epsilon P(\gamma + \delta\beta P)}{1 + \beta P} + \frac{\epsilon NP}{P + N} + d_2 P_{xx}, \quad (4)$$

on the one-dimensional space domain $\Omega = (0,1)$ with the positive initial conditions and the boundary conditions

$$N_x(0,t) = N_x(1,t) = P_x(0,t) = P_x(1,t) = 0. \quad (5)$$

In this paper, we present an efficient and accurate numerical method for solving Eqs. (3) and (4). The scheme preserves the positivity and boundedness of the numerical solutions depending only on the temporal, but not on the spatial step sizes. We perform numerical experiments to demonstrate the robustness and accuracy of the numerical solution for the Turing instability.

This paper is organized as follows. In Sec. 2, we briefly review the model analysis in the kinetic system and the diffusion–reaction system to observe the stationary solution. In Sec. 3, we propose the efficient and accurate numerical scheme for the predator–prey model. Moreover, we analyze and prove the positivity and boundedness of numerical solutions. In Sec. 4, we illustrate the numerical solutions with respect to the Turing instability region and we carry out some evidences for the numerical nonconstant stationary solution with amplitudes as time evolves. And we calculate the stability constraint for an explicit scheme comparing with our semi-implicit scheme. Conclusions are drawn in Sec. 5.

## 2. Preliminaries

In this section, we review the equilibrium solution in the kinetic system, the necessary conditions for the Turing instability, and the nonconstant stationary solution in reaction–diffusion systems.

In the kinetic system (i.e. $d_1 = d_2 = 0$), we get the equilibrium points by setting the time derivative term as zero. Then the equilibrium points are $(0,0)$, $(1,0)$, and at least one point has positive values which is the point of intersection of the null-clines as shown in Fig. 1. The prey and predator's null-clines are

$$P = H_1(N) = \frac{(1 - N)N}{\alpha - 1 + N},$$

$$P = H_2(N) = \frac{-\gamma - \beta(\delta - 1)N + \sqrt{[\gamma + \beta(\delta - 1)N]^2 + 4\delta\beta(-\gamma + 1)N}}{2\beta\delta},$$

respectively.

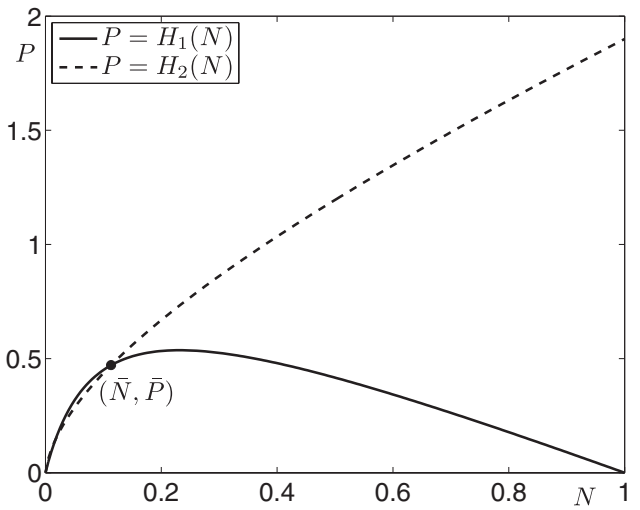


Fig. 1. Null-clines of $N$ and $P$ with $\epsilon = 1$, $\alpha = 1.1$, $\gamma = 0.05$, $\beta = 1$, and $\delta = 0.5$.

Let $(\overline{N}, \overline{P})$ be an equilibrium point with positive values, then $(\overline{N}, \overline{P})$ is in the Allée effect zone [Stephens *et al.*, 1999] as shown in Fig. 1. To observe the local stability near $(\overline{N}, \overline{P})$, let $u = N - \overline{N}$ and $v = P - \overline{P}$. Then when we let

$$f(N,P) = N(1-N) - \frac{\alpha NP}{P+N},$$

$$g(N,P) = \epsilon P\left(-\frac{\gamma + \beta\delta P}{1+\beta P}\right) + \frac{\beta NP}{P+N},$$

with the Jacobian matrix $A$, the linearized kinetic system forms

$$\begin{pmatrix} u_t \\ v_t \end{pmatrix} = A \begin{pmatrix} u \\ v \end{pmatrix}, \quad \text{where}$$

$$A = \begin{pmatrix} f_N(\overline{N},\overline{P}) & f_P(\overline{N},\overline{P}) \\ g_N(\overline{N},\overline{P}) & g_P(\overline{N},\overline{P}) \end{pmatrix} = \begin{pmatrix} a_{11} & a_{12} \\ a_{21} & a_{22} \end{pmatrix}.$$

Therefore in the kinetic system, $(\overline{N}, \overline{P})$ is locally asymptotically stable when trace $A < 0$ and det $A > 0$, that is, $a_{11} + a_{22} < 0$ and $a_{11}a_{22} - a_{12}a_{21} > 0$.

Then, we consider the Turing instability occurring conditions and the nonconstant stationary solutions. Let the two-dimensional vector $\mathbf{u} = (N, P)^T$, the diagonal matrix $D = \text{diag}(d_1, d_2)$, and $F = (f, g)^T$. Then Eqs. (3)–(5) can be rewritten as

$$\mathbf{u}_t = F(\mathbf{u}) + D\mathbf{u}_{xx}, \tag{6}$$

$$\mathbf{u}_x(0,t) = \mathbf{u}_x(1,t) = \mathbf{0}. \tag{7}$$

The equilibrium $\overline{\mathbf{u}} = (\overline{N}, \overline{P})$ is called Turing unstable, if it is an asymptotically stable equilibrium of the kinetic system but it is unstable with diffusion term [Cavani & Farkas, 1994a, 1994b]. Here, a linear analysis is reviewed as a general method for deriving the necessary condition of the Turing instability [Cavani & Farkas, 1994a, 1994b; Lizana & Marín, 2005; Aly *et al.*, 2011]. Using a method of separation variables and eigenvalue problem, the eigenvalues are $\lambda_n = (n\pi)^2$, $n = 0, 1, 2, \ldots$, and their corresponding eigenfunctions are $\psi_n(x) = \cos(n\pi x)$, $n = 0, 1, 2, \ldots$ of the linearized system of Eqs. (6) and (7).

Let $B_n = A - \lambda_n D$. With the stable condition in the kinetic system, the equilibrium solution $(\overline{N}, \overline{P})$ is Turing unstable when $d_1 a_{22} + d_2 a_{11} > 0$ and $(d_1 a_{22} + d_2 a_{11})^2 - 4 d_1 d_2 \det A > 0$ or there exists a positive integer $k$ such that $\det B_k < 0$. We fix $d_1$ and take $d_2$ as a bifurcation parameter. For $\overline{\mathbf{u}} = (\overline{N}, \overline{P})^T$, we have $F(\overline{\mathbf{u}}) = \mathbf{0}$ for all $d_2 \in [0, \infty)$. Let $d^*$ be the critical value for a Turing bifurcation.

We say that $\overline{\mathbf{u}}$ undergoes a Turing bifurcation at $d^* \in [0, \infty)$ if the solution $\overline{\mathbf{u}}$ is asymptotically stable for $0 < d_2 < d^*$, it is unstable for $d^* < d_2$, and Eq. (6) has a nonconstant stationary solution in some neighborhood of $d^*$. To find $d^*$, we consider the eigenvalues of $B_n$. The critical value for a Turing bifurcation $d^*$ is as follows with $a_{11}/\lambda_2 \le d_1 < a_{11}/\lambda_1$ [Aly *et al.*, 2011]:

$$d^* = \frac{\det A - \lambda_1 d_1 a_{22}}{\lambda_1(a_{11} - \lambda_1 d_1)}. \tag{8}$$

When $d_2 = d^*$, the eigenvalues are zero and trace $B_n$. Since trace $B_n < 0$, we consider the zero eigenvalue. Denote a unit eigenvector corresponding to the zero eigenvalue by $(\eta_1, \eta_2)^T$. Then a Turing unstable solution of the linearlized system of Eqs. (6) and (7) forms

$$\phi(x) = \begin{pmatrix} \eta_1 \\ \eta_2 \end{pmatrix} \cos(\pi x).$$

For the nonlinear Eqs. (6) and (7), by the bifurcation from a simple eigenvalue theorem [Smoller, 1991], $d^*$ is a bifurcation point and there exists a $\delta > 0$ satisfying a function $d_2(s) : (-\delta, \delta) \to R$ such that

$$\mathbf{u}(x) = \overline{\mathbf{u}} + s\phi(x)\cos(\pi x) + O(s^2). \tag{9}$$

Then such $\mathbf{u}(x)$ is the nonconstant stationary solution of the nonlinear parabolic system. If we rewrite

the above equation in the component form, then

$$N(x) = \overline{N} + s\eta_1 \cos(\pi x) + O(s^2),$$
$$P(x) = \overline{P} + s\eta_2 \cos(\pi x) + O(s^2).$$

By the theorem in [Smoller, 1991; Aly *et al.*, 2011], Eqs. (6) and (7) have no other stationary solutions except $(\overline{N}, \overline{P})$ and Eq. (9).

## 3. Numerical Approach

In this section, we propose an efficient and accurate numerical scheme. Moreover, we prove the positiveness and boundedness of the scheme which depends only on temporal not on spatial step sizes.

### 3.1. *Proposed numerical scheme*

Let us first discretize the given computational space domain $\Omega = (0, 1)$ as a uniform grid with a space step $h = 1/N_x$ and a time step $\Delta t = T/N_t$. The numerical approximation to the solution $(\overline{N}, \overline{P})$ is denoted by

$$N_i^n \equiv N(x_i, t^n) = N((i - 0.5)h, n\Delta t),$$
$$P_i^n \equiv P(x_i, t^n) = P((i - 0.5)h, n\Delta t),$$

where $i = 1, 2, \ldots, N_x$ and $n = 0, 1, \ldots, N_t$. We will solve Eqs. (3) and (4) using the semi-implicit scheme in time and a centered difference scheme in space. Since fully explicit schemes may have restriction of time step by diffusion term and fully implicit schemes may be expensive [Ruuth, 1995], it is efficient to use the semi-implicit scheme. We write the schemes as follows:

$$\frac{N_i^{n+1} - N_i^n}{\Delta t} = N_i^n \left(1 - N_i^n - \frac{\alpha P_i^n}{P_i^n + N_i^n}\right) + d_1 \Delta_h N_i^{n+1}, \tag{10}$$

$$\frac{P_i^{n+1} - P_i^n}{\Delta t} = \epsilon P_i^n \left(-\frac{\gamma + \delta\beta P_i^n}{1 + \beta P_i^n} + \frac{N_i^n}{P_i^n + N_i^n}\right) + d_2 \Delta_h P_i^{n+1} \tag{11}$$

for $i = 1, \ldots, N_x$ and $n = 0, \ldots, N_t - 1$.

Assume that the initial condition of $N$ satisfies $0 < N(x, 0) \leq 1$ and $P$ satisfies $0 < P(x, 0) \leq L$ for all $x$, where $L = \max(1/\gamma, Q)$ for some positive $Q > 1/\gamma$. For the boundary condition, Neumann condition is applied:

$$N_0^n = N_1^n, \quad N_{N_x+1}^n = N_{N_x}^n,$$
$$P_0^n = P_1^n, \quad P_{N_x+1}^n = P_{N_x}^n.$$

Since we discretize the system as a nonlinear term explicitly and a linear term implicitly, it is convenient to split the scheme into following two steps.

***Step 1***

$$\frac{N_i^* - N_i^n}{\Delta t} = N_i^n \left(1 - N_i^n - \frac{\alpha P_i^n}{P_i^n + N_i^n}\right), \tag{12}$$

$$\frac{P_i^* - P_i^n}{\Delta t} = \epsilon P_i^n \left(-\frac{\gamma + \delta\beta P_i^n}{1 + \beta P_i^n} + \frac{N_i^n}{P_i^n + N_i^n}\right). \tag{13}$$

***Step 2***

$$\frac{N_i^{n+1} - N_i^*}{\Delta t} = d_1 \frac{N_{i-1}^{n+1} - 2N_i^{n+1} + N_{i+1}^{n+1}}{h^2}, \tag{14}$$

$$\frac{P_i^{n+1} - P_i^*}{\Delta t} = d_2 \frac{P_{i+1}^{n+1} - 2P_i^{n+1} + P_{i-1}^{n+1}}{h^2}. \tag{15}$$

### 3.2. *The positiveness and boundedness of the solution under certain condition of $\Delta t$*

Now we will show the positiveness and boundedness of the solution under the certain condition of $\Delta t$. Suppose that $0 < N_i^n \leq 1$, $0 < P_i^n \leq L$ for $i = 1, \ldots, N_x$, and $L = \max(1/\gamma, Q)$ for some positive $Q$.

Firstly, for the nonlinear term of Step 1, we show the positiveness and boundedness of $N_i^*$ and $P_i^*$ for $i = 1, \ldots, N_x$.

$$\begin{aligned} N_i^* &= N_i^n + \Delta t N_i^n \left(1 - N_i^n - \frac{\alpha P_i^n}{P_i^n + N_i^n}\right) \\ &\geq N_i^n + \Delta t N_i^n (1 - N_i^n) - \Delta t \alpha N_i^n \\ &\geq N_i^n - \Delta t \alpha N_i^n = (1 - \Delta t \alpha) N_i^n > 0 \end{aligned}$$

when $\Delta t < 1/\alpha$. And with $\Delta t \leq 1$

$$\begin{aligned} N_i^* &= N_i^n + \Delta t N_i^n \left(1 - N_i^n - \frac{\alpha P_i^n}{P_i^n + N_i^n}\right) \\ &\leq N_i^n + \Delta t N_i^n (1 - N_i^n) \leq N_i^n + \Delta t (1 - N_i^n) \\ &= N_i^n (1 - \Delta t) + \Delta t \leq 1 - \Delta t + \Delta t = 1. \end{aligned}$$

For $P^*$, we have

$$\begin{aligned} P_i^* &= P_i^n + \Delta t\epsilon P_i^n\left(-\frac{\gamma+\delta\beta P_i^n}{1+\beta P_i^n} + \frac{N_i^n}{P_i^n+N_i^n}\right) \\ &\geq P_i^n + \Delta t\epsilon P_i^n\left(-\delta + \frac{\delta-\gamma}{1+\beta P_i^n}\right) \\ &\geq P_i^n\left(1-\Delta t\epsilon\frac{\gamma+\delta\beta}{1+\beta}\right) > 0 \end{aligned}$$

when $\Delta t < (1+\beta)/(\epsilon\gamma+\epsilon\delta\beta)$. And using $0<\gamma\leq\delta$, we get

$$\begin{aligned} P_i^* &= P_i^n + \Delta t\epsilon P_i^n\left(-\frac{\gamma+\delta\beta P_i^n}{1+\beta P_i^n} + \frac{N_i^n}{P_i^n+N_i^n}\right) \\ &\leq P_i^n + \Delta t\epsilon P_i^n\left(-\frac{\gamma+\gamma\beta P_i^n}{1+\beta P_i^n} + \frac{1}{P_i^n}\right) \\ &= P_i^n - \Delta t\epsilon P_i^n\gamma + \Delta t\epsilon \\ &= P_i^n(1-\Delta t\epsilon\gamma) + \Delta t\epsilon \\ &\leq L(1-\Delta t\epsilon\gamma) + \Delta t\epsilon \\ &= L + \Delta t\epsilon\gamma\left(\frac{1}{\gamma} - L\right) \leq L \end{aligned}$$

for all $\Delta t$. By these results, for Eqs. (12) and (13), if $0<N_i^n\leq 1$, $0<P_i^n\leq L$ for $i=0,\ldots,N_x$ and $\Delta t<\min(1,1/\alpha,(1+\beta)/(\epsilon\gamma+\epsilon\delta\beta))$, then

$$0<N_i^*\leq 1, \quad 0<P_i^*\leq L \quad \text{for } i=1,\ldots,N_x.$$

Secondly, for the linear term of Step 2, we need to show the boundedness and positiveness of $N_i^{n+1}$ and $P_i^{n+1}$ for $i=1,\ldots,N_x$. So we need to show the following:

$$\begin{cases} N_i^{n+1}\geq m^*>0, & \text{where } m^*=\min\limits_{1\leq k\leq N_x} N_k^* \\ N_i^{n+1}\leq M^*\leq 1, & \text{where } M^*=\max\limits_{1\leq k\leq N_x} N_k^* \\ P_i^{n+1}\geq m'^*>0, & \text{where } m'^*=\min\limits_{1\leq k\leq N_x} P_k^* \\ P_i^{n+1}\leq M'^*\leq L, & \text{where } M'^*=\max\limits_{1\leq k\leq N_x} P_k^*. \end{cases} \tag{16}$$

To show the first inequality of Eq. (16), assume to the contrary that $N_i^{n+1}<m^*$, then there exists some $i$, $2\leq i\leq N_x-1$ which satisfies $N_i^{n+1}\leq\min(N_{i-1}^{n+1},N_{i+1}^{n+1})$. Let $\omega=d_1\Delta t/h^2$. Then Eq. (14) can be written as

$$(1+2\omega)N_i^{n+1} = N_i^* + \omega\big(N_{i-1}^{n+1}+N_{i+1}^{n+1}\big).$$

Since $N_i^{n+1}<N_i^*$ by the assumption, we rewrite the above equation as $N_i^{n+1}>(N_{i-1}^{n+1}+N_{i+1}^{n+1})/2$, and which implies that either $N_i^{n+1}>N_{i-1}^{n+1}$ or $N_i^{n+1}>N_{i+1}^{n+1}$. But since it contradicts the assumption, we have $N_i^{n+1}\geq m^*$. For the case of $i=1$, assume $N_1^{n+1}<m^*$ such that $N_1^{n+1}\leq N_2^{n+1}$, then using the homogeneous Neumann boundary condition $N_0^{n+1}=N_1^{n+1}$, we have $(1+\omega)N_1^{n+1}=N_1^*+\omega N_2^{n+1}$. Therefore, we have $N_1^{n+1}>N_2^{n+1}$, which contradicts our assumption. In the case of $N_{N_x}^{n+1}<m^*$ and $N_{N_x}^{n+1}\leq N_{N_x-1}^{n+1}$, the same result holds with the same reasoning.

And we show the second inequality of Eq. (16). Assume contrary as $N_i^{n+1}>M^*$ such that $N_i^{n+1}\geq\max(N_{i-1}^{n+1},N_{i+1}^{n+1})$ for some $i$, $2\leq i\leq N_x-1$. Then Eq. (14) is $(1+2\omega)N_i^{n+1}=N_i^*+\omega(N_{i-1}^{n+1}+N_{i+1}^{n+1})$.

Therefore we have $N_i^{n+1}<(N_{i-1}^{n+1}+N_{i+1}^{n+1})/2$ by the assumption, which implies that either $N_i^{n+1}<N_{i-1}^{n+1}$ or $N_i^{n+1}<N_{i+1}^{n+1}$, which contradicts the assumption. So, we have $N_i^{n+1}\leq M^*$. For the case of $i=1$ and $N_x$, we can show the inequality applying the same argument as before. Also, using the similar argument the third and the fourth inequalities of Eq. (14) can be proved. Collecting all the above results, we get the following theorem:

**Theorem.** *Let $0<N_i^0\leq 1$, $0<P_i^0\leq L$ for $i=1,\ldots,N_x$ where $L=\max\{1,Q\}$ for some positive $Q$. Suppose that*

$$\Delta t\leq\min\left(1,\frac{1}{\alpha},\frac{1+\beta}{\epsilon(\gamma+\delta\beta)}\right).$$

*Then the numerical solutions $N_i^{n+1}$ and $P_i^{n+1}$ obtained from the schemes (10) and (11) satisfy the positiveness and boundedness*:

$$0<N_i^{n+1}\leq 1, \quad 0<P_i^{n+1}\leq L \quad \text{for } i=1,\ldots,N_x \text{ and } n=0,1,\ldots.$$

## 4. Numerical Results

In this section, we investigate the numerical solutions with stable and unstable bifurcation parameters $d_2$. Then we perform numerical experiments for nonconstant stationary solutions with small amplitudes. Moreover, we exhibit the effect of amplitudes on the equilibrium solutions. Finally,

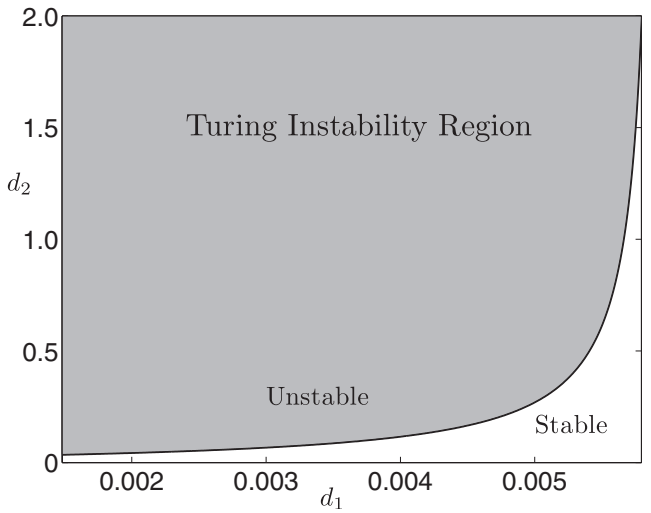


Fig. 2. The phase plane of the prey diffusion $d_1$ and the predator diffusion $d_2$.

we compare our proposed method with a standard explicit scheme.

### 4.1. *Numerical solutions with Turing instability*

In numerical tests, we use the same parameters as in [Aly *et al.*, 2011]: $\epsilon = 1$, $\alpha = 1.1$, $\gamma = 0.05$, $\beta = 1$, and $\delta = 0.5$ on the computational domain $\Omega = (0, 1)$. In Fig. 2, Turing instability region is shown in the phase plane of diffusion coefficients $d_1$ and $d_2$ using Eq. (8).

For diffusion coefficients, we can consider $d_1$ as an activator and $d_2$ as an inhibitor in the activator–inhibitor system. In terms of the activator–inhibitor mechanism by Murray [2003], the inhibitor must diffuse faster than the activator, that is $d_1 < d_2$. Therefore we take a small value for $d_1 = 0.005$. The initial conditions are given as

$$N(x, 0) = \overline{N} + 0.0214 \cos(\pi x), \tag{17}$$

$$P(x, 0) = \overline{P} + 0.0066 \cos(\pi x), \tag{18}$$

where $(\overline{N}, \overline{P}) = (0.113585, 0.471397)$ is the unique stable equilibrium point. We compare the numerical solutions with $d_2$ in the stable and unstable regions as shown in Fig. 3. We use the spatial mesh size $h = 0.005$, the time step $\Delta t = 0.9$, and the total time $T = 1000$. In case of $d_2 < d^*$ ($d_2 = 0.2$ and $d^* = 0.271$), the time evolutions of $N(x, t)$ and $P(x, t)$ are shown in Figs. 3(a) and 3(b), respectively. The numerical solutions converge to the equilibrium solution $\overline{N}$ and $\overline{P}$ as time iterations increase. However, in case of $d_2 > d^*$ ($d_2 = 0.32$), the time evolution of $N(x, t)$ and $P(x, t)$ are shown in Figs. 3(c) and 3(d), respectively. The numerical solutions show the deviation from the equilibrium solution $\overline{N}$ and $\overline{P}$ since $d_2$ is in the Turing instability region.

### 4.2. *Nonconstant stationary solution*

In this section, we investigate numerically nonconstant stationary solutions with small amplitudes. Let $(\eta_1, \eta_2)^T$ be the unit eigenvector corresponding to the zero eigenvalue of $B_1$. We use the spatial mesh size $h = 0.01$ with the time step $\Delta t = 0.01$,

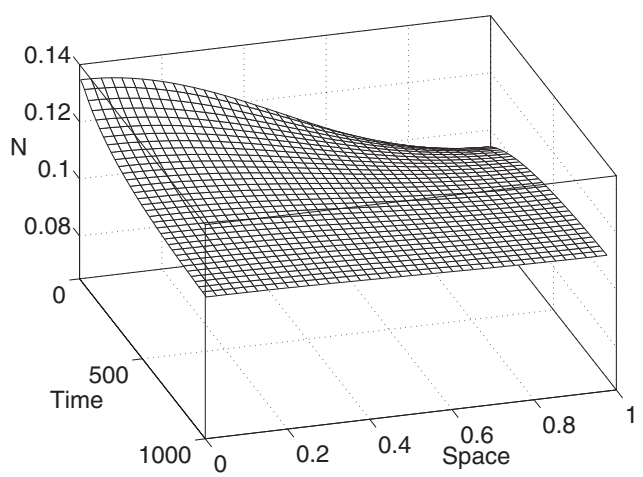


(a)

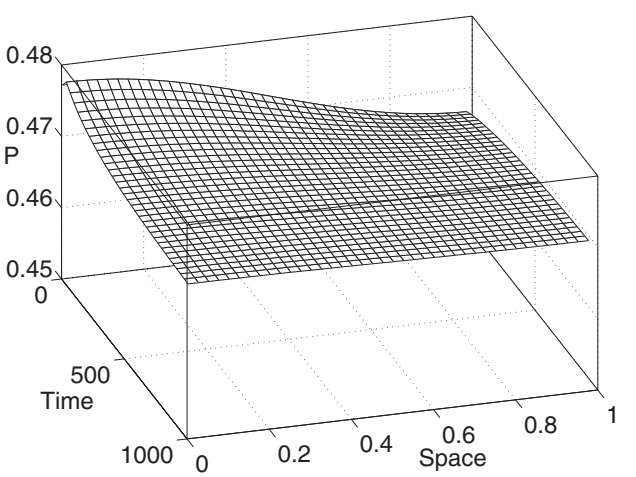


(b)

Fig. 3. $(d_1, d_2) = (0.005, 0.2)$, which is in stable region: (a) the prey solution $N(x, t)$ and (b) the predator solution $P(x, t)$. $(d_1, d_2) = (0.005, 0.32)$, which is in unstable region: (c) the prey solution $N(x, t)$ and (d) the predator solution $P(x, t)$.

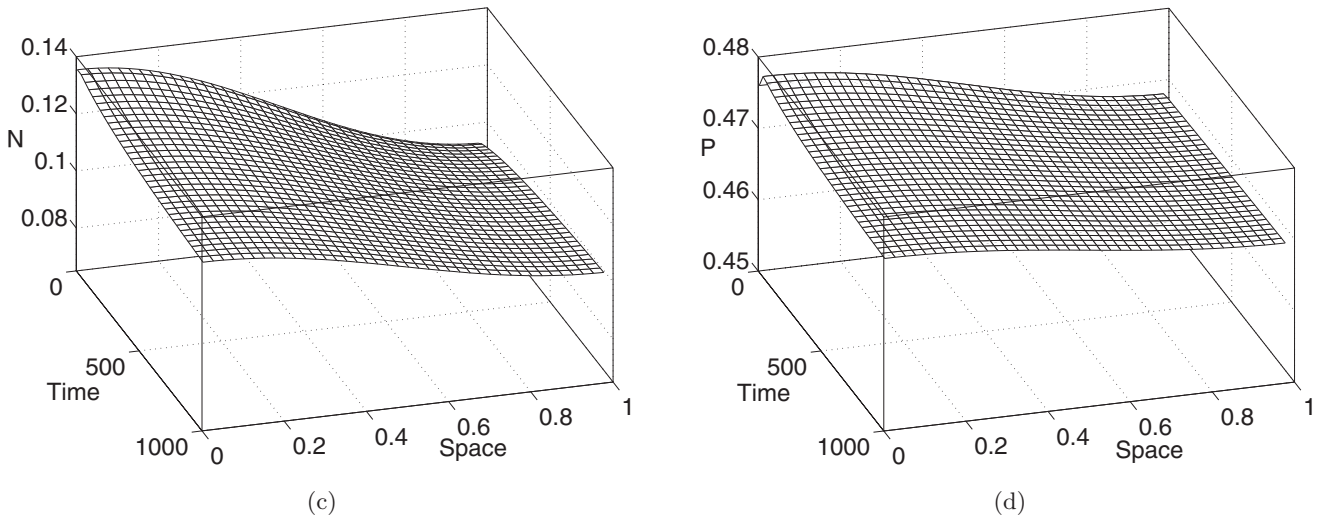


(c) (d)

Fig. 3. (*Continued*)

and the final time $T = 100$. Initial conditions are taken close to the nonconstant stationary solutions,

$$N(x,0) = \overline{N} + s\eta_1 \cos(\pi x), \tag{19}$$

$$P(x,0) = \overline{P} + s\eta_2 \cos(\pi x), \tag{20}$$

where we take $s$ as $0.002, 0.004, 0.008$, and $0.016$. Figures 4 and 5 show the prey and predator's nonconstant stationary numerical solutions with different $s$ values in two cases of $d_2 < d^*$ and $d_2 > d^*$, respectively. Symbols, $\circ$, $\diamond$, $\square$ and $\triangledown$, are the initial conditions with increased values of $s$, respectively. Solid, dashed, dash-doted, and dotted lines are corresponding numerical equilibrium solutions. This result demonstrates that the initially given nonconstant stationary solution is the numerical nonconstant stationary solution when $s$ is small.

The following test in Fig. 6 demonstrates the existence of the numerical nonconstant equilibrium solution after long time evolution. Figures 6(a) and 6(c) show the time evolution of prey and predator solutions with $d_1 = 0.005$, $d_2 = 0.27$, $d^* = 0.271$, and $s = 0.016$. We use the spatial mesh size $h = 0.0025$, the time step $\Delta t = 0.01$, and the final time $T = 100$. And Figs. 6(b) and 6(d) show temporal evolutions of prey and predator solutions at five points ($x = 0.00125$, 0.24875, 0.49875, 0.74875, 0.99875). At each point $x$, Fig. 6 shows that with

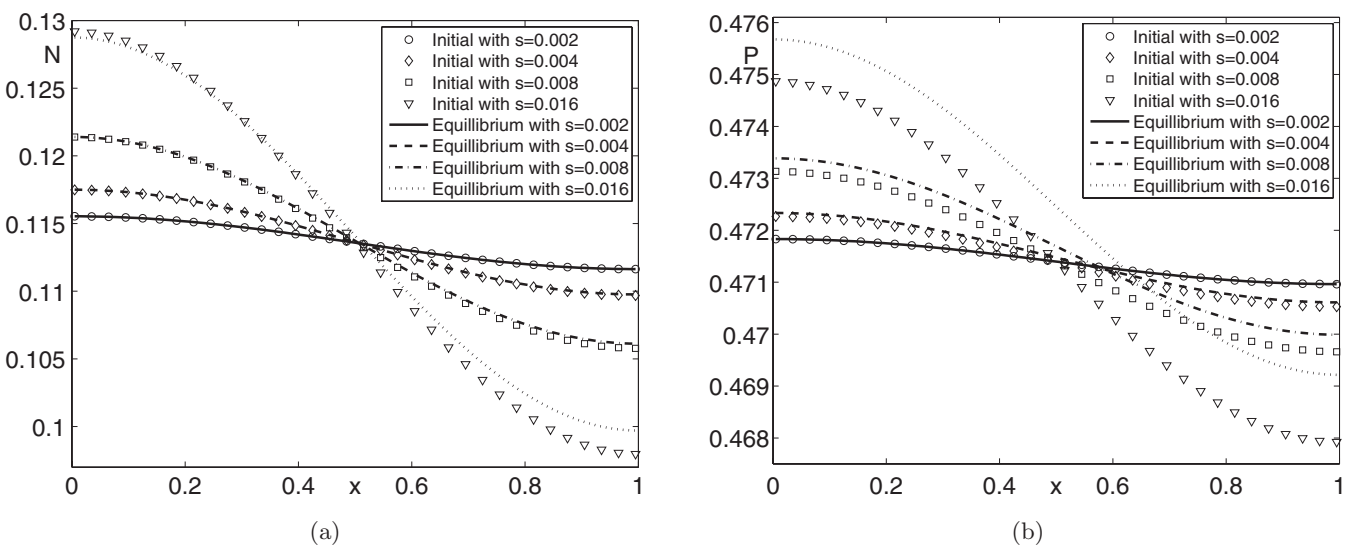


(a) (b)

Fig. 4. $d_2 < d^*$ with different $s$: (a) prey $N(x,t)$ and (b) predator $P(x,t)$ solution pattern ($d_1 = 0.005, d_2 = 0.27, d^* = 0.271$). Here, each marker represents the initial condition depending on $s$.

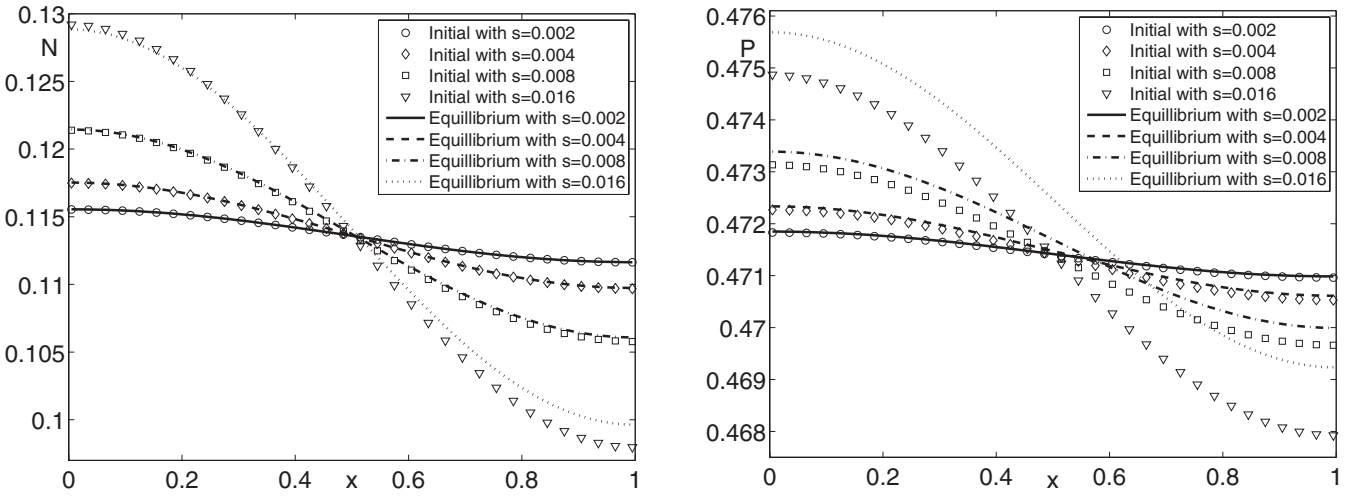


(a) (b)

Fig. 5. $d_2 > d^*$ with different $s$: (a) prey $N(x,t)$ and (b) predator $P(x,t)$ solution pattern ($d_1 = 0.005$, $d_2 = 0.272$, $d^* = 0.271$). Here, each marker represents the initial condition depending on $s$.

small amplitude $s$, the pattern of the numerical solution goes to the stationary solution.

### 4.3. *Effect of the amplitudes*

Figures 4 and 5 show similar results when the values of $d_2$ are close enough to the Turing bifurcation point $d^*$. Therefore in this section, we let $d_2 = d^*$ to consider the solution patterns on the bifurcation point. To observe the effect of amplitudes on the stationary state, the following tests are presented. The procedure is repeated until the relative change with respect to a time step $\Delta t$ is smaller than a tolerance $\epsilon$, namely

$$\max\left(\frac{\|N^{n+1} - N^n\|_\infty}{\Delta t}, \frac{\|P^{n+1} - P^n\|_\infty}{\Delta t}\right) < \epsilon.$$

In this test, we use time step $\Delta t = 0.9$, space step $h = 0.01$, tolerance $\epsilon = 1.0E{-}6$, and the other parameters as the same values as in the previous tests, with initial conditions as Eqs. (17) and (18).

Figures 7(a), 7(c) and 7(b), 7(d) show the solution patterns of $N(x,t)$ (the first row) and $P(x,t)$ (the second row) with small amplitudes $s = 0.002$,

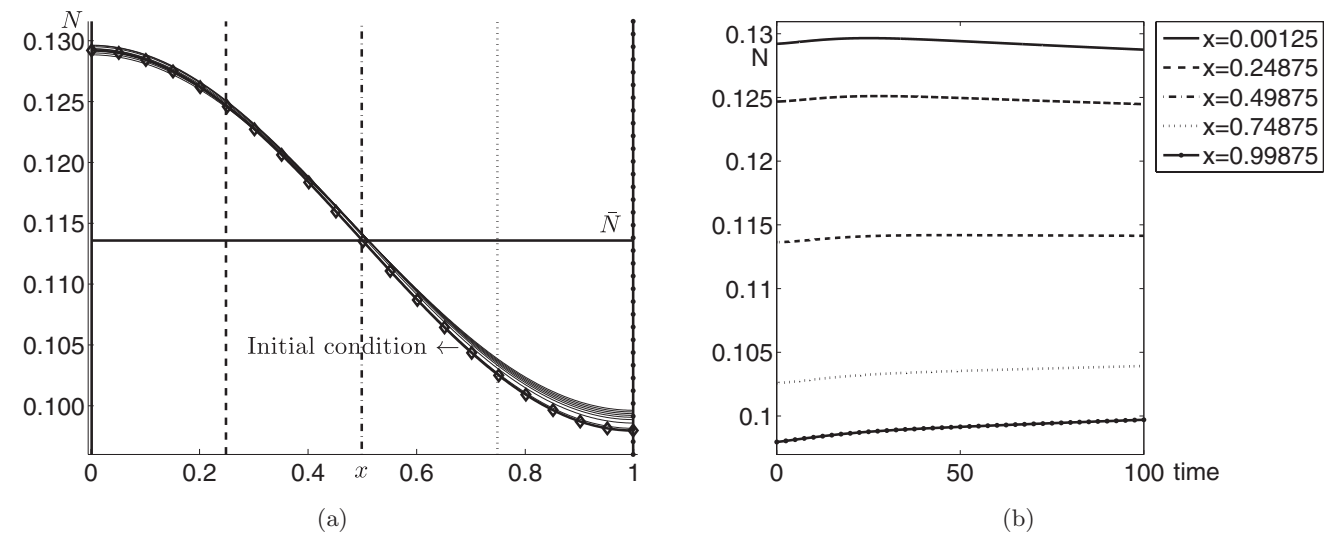


(a) (b)

Fig. 6. (a) and (c) The time evolution of prey and predator solution pattern $N(x,t)$, $P(x,t)$ with $d_1 = 0.005$, $d_2 = 0.27$, $d^* = 0.271$ and $s = 0.016$. (b) and (d) Prey and predator solution at five points ($x = 0.00125$, 0.24875, 0.49875, 0.74875, 0.99875) depending on the time.

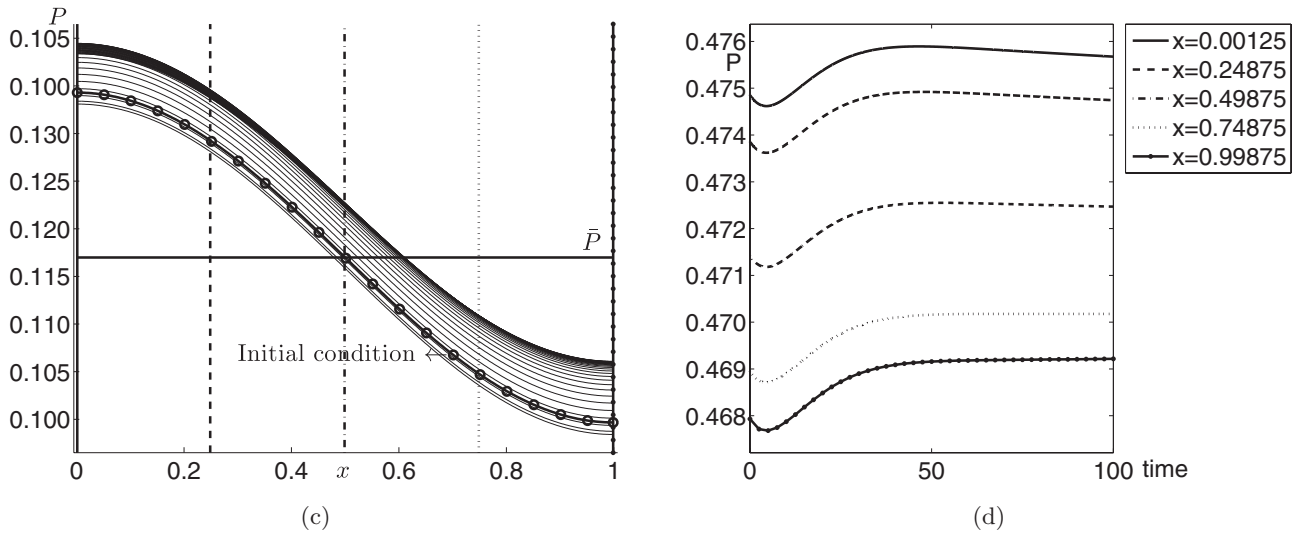


(c) (d)

Fig. 6. (*Continued*)

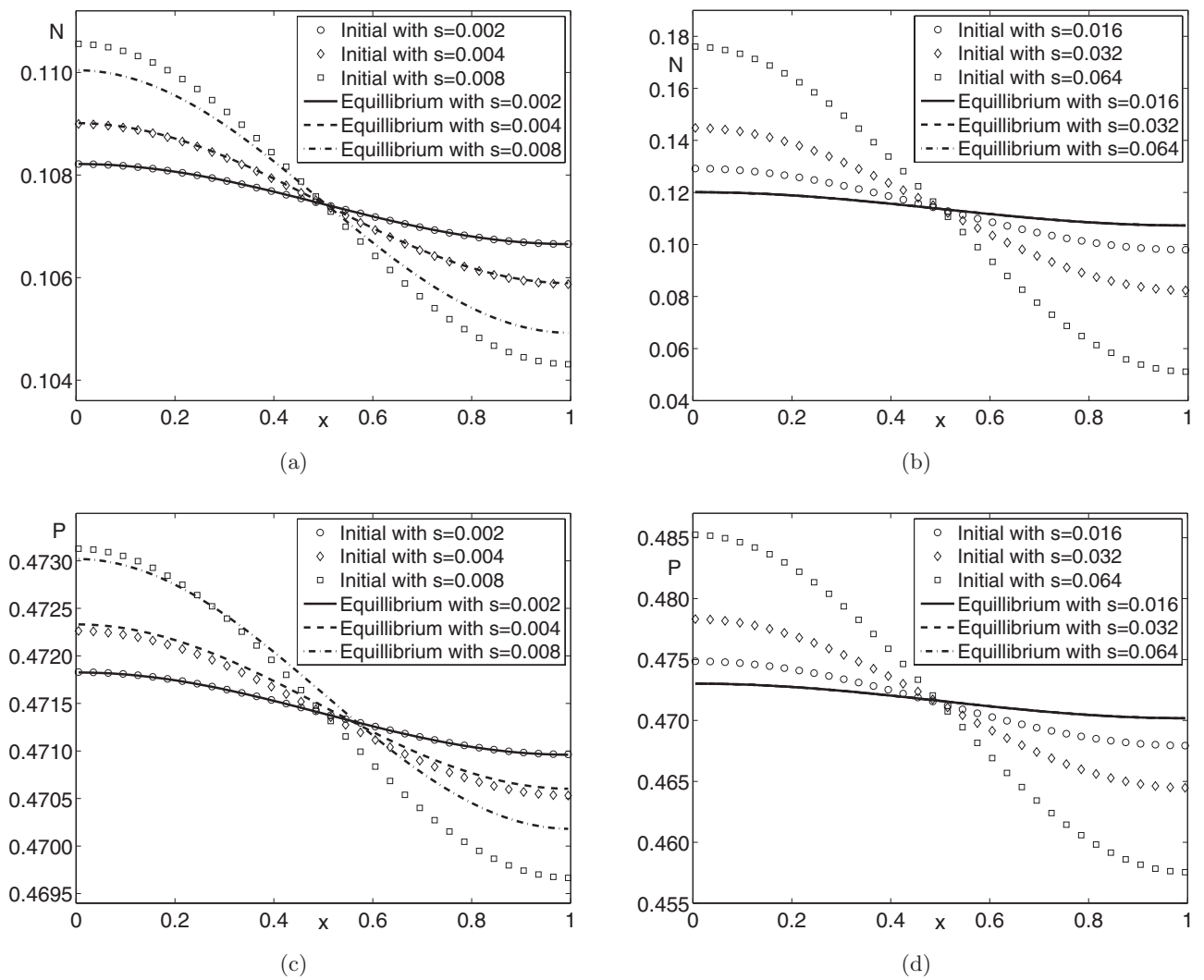


(a) (b)

(c) (d)

Fig. 7. $d_1 = 0.005$ and $d_2 = d^* = 0.271$ with different $s$: (a) and (c) $s = 0.002$, 0.004, 0.008, (b) and (d) $s = 0.016$, 0.032, 0.064, where the first and second rows are $N(x,t)$ and $P(x,t)$ solutions, respectively. Here, each marker represents the initial condition with different $s$.

Table 1. Comparison of stability constraints for an explicit and the proposed scheme.

| Mesh Size | Explicit Scheme | Proposed Scheme |
|---|---|---|
| $h = 0.01$ | $\Delta t \leq 1.853E{-}4$ | $\Delta t \leq 1.545E{+}1$ |
| $h = 0.005$ | $\Delta t \leq 4.630E{-}5$ | $\Delta t \leq 1.545E{+}1$ |
| $h = 0.0025$ | $\Delta t \leq 1.150E{-}5$ | $\Delta t \leq 1.545E{+}1$ |
| $h = 0.00125$ | $\Delta t \leq 2.800E{-}6$ | $\Delta t \leq 1.545E{+}1$ |
| $h = 0.000625$ | $\Delta t \leq 7.000E{-}7$ | $\Delta t \leq 1.545E{+}1$ |

0.004, 0.008 and with large enough amplitudes $s =$ 0.016, 0.032, 0.064, respectively. These results suggest that the solutions converge to the same nonconstant solution when $s$ is large enough as shown in Figs. 7(b) and 7(d).

### 4.4. *Stability test*

Finally, we investigate the stability constraint for an explicit and the proposed schemes. We calculate the maximum $\Delta t$ corresponding to different spatial grid sizes $h$ so that stable solutions can be computed up to the total iteration 10 000. We use the following parameters: $d_1 = 0.005$, $d_2 = d^* = 0.271$, and $s = 0.032$ with initial conditions Eqs. (19) and (20). The results in Table 1 indicate that the explicit scheme has a stability restriction of the time step, $\Delta t \approx O(h^2)$. Whereas the proposed scheme is only restricted by the time step, $\Delta t$ given in Sec. 3.2 is as follows:

$$\Delta t \leq \min\left(1, \frac{1}{\alpha}, \frac{1+\beta}{\epsilon(\gamma + \delta\beta)}\right) \approx 0.9091,$$

which is independent of spatial step sizes $h$. Therefore, the proposed semi-implicit scheme is practically more stable than the explicit scheme.

## 5. Conclusions

We have presented an efficient and accurate numerical method for solving a ratio-dependent predator–prey model with a Turing instability. The system was discretized by a finite difference method with a semi-implicit scheme which allows much larger time step sizes than those required by a standard explicit scheme. We have proved the positivity and boundedness of the numerical solutions depending only on the temporal, but not on the spatial step sizes. We performed numerical experiments demonstrating the robustness and accuracy of the numerical solution for the Turing instability. In particular, we showed that the numerical nonconstant stationary solutions exist. We also performed numerical stability test and the result showed that our proposed scheme is a practically unconditionally stable scheme. That is, it has only a time step size constraint. Since our proposed scheme assures the stability, we expect that the proposed scheme is useful to investigate the biological system numerically with very fine spatial grids.

## Acknowledgments

This work was supported by National Junior research fellowship from the National Research Foundation of Korea grant funded by the Korea government (No. 2011-0012258). The authors also wish to thank the reviewers for the constructive and helpful comments on the revision of this article.

## References

Aly, S., Kim, I. & Sheen, D. [2011] "Turing instability for a ratio-dependent predator–prey model with diffusion," *Appl. Math. Comput.* **217**, 7265–7281.

Arditi, R. & Ginzburg, L. R. [1989] "Coupling in predator–prey dynamics: Ratio-dependence," *J. Theor. Biol.* **139**, 311–326.

Calude, C. S. & Păun, G. [2004] "Bio-steps beyond Turing," *BioSyst.* **77**, 175–194.

Cavani, M. & Farkas, M. [1994a] "Bifurcations in a predator–prey model with memory and diffusion. I: Andronov–Hopf bifurcation," *Acta Math. Hungar.* **63**, 213–229.

Cavani, M. & Farkas, M. [1994b] "Bifurcations in a predator–prey model with memory and diffusion. II: Turing bifurcation," *Acta Math. Hungar.* **63**, 375–393.

Holling, C. S. [1959] "Some characteristics of simple types of predation and parasitism," *Can. Entomol.* **91**, 385–398.

Kuang, Y. & Beretta, E. [1998] "Global qualitative analysis of a ratio-dependent predator–prey system," *J. Math. Biol.* **36**, 389–406.

Lizana, M. & Marín, V. J. J. [2005] "Pattern formation in a reaction diffusion ratio-dependent predator–prey model," *Notas de Mathemática* **239**, 1–16.

McGehee, E. A., Schutt, N., Vasquez, D. A. & Peacock-Lopez, E. [2008] "Bifurcations and temporal and spatial patterns of a modified Lotka–Voltera model," *Int. J. Bifurcation and Chaos* **18**, 2223–2248.

Medvinsky, A. B., Petrovskii, S. V., Tikhonova, I. A., Malchow, H. & Li, B. L. [2002] "Spatiotemporal complexity of plankton and fish dynamics," *SIAM Rev.* **44**, 311–370.

Murray, J. D. [2003] *Mathematical Biology II: Spatial Models and Biomedical Applications* (Springer, Berlin).

Nakao, H. & Mikhailov, A. S. [2010] "Turing patterns in network-organized activator-inhibitor systems," *Nature Phys.* **6**, 544–550.

Peng, G. J., Jiang, Y. L. & Li, C. P. [2009] "Bifurcations of a Holling-type II predator–prey system with constant rate harvesting," *Int. J. Bifurcation and Chaos* **19**, 2499–2514.

Ruuth, S. J. [1995] "Implicit-explicit methods for reaction-diffusion problems in pattern formation," *J. Math. Biol.* **34**, 148–176.

Shiferaw, Y. & Karma, A. [2006] "Turing instability mediated by voltage and calcium diffusion in paced cardiac cells," *Nat. Acad. Sci.* **103**, 5670–5675.

Smoller, J. [1991] *Shock Waves and Reaction-Diffusion Equations* (Springer-Verlag, Berlin).

Stephens, P. A., Sutherland, W. J. & Freckleton, R. P. [1999] "What is the Allee effect?" *Oikos* **87**, 185–190.

Tapaswi, P. K. & Chattopadhyay, J. [1993] "Turing structure during embryogenesis," *BioSyst.* **29**, 25–36.

Wang, W., Liu, Q. & Jin, Z. [2007] "Spatiotemporal complexity of a ratio-dependent predator–prey system," *Phys. Rev. E* **75**, 051913.